A Computationally Efficient Algorithm for Rotor Design Optimization of Synchronous Reluctance Machines

M. H. Mohammadi[1], T. Rahman[2], R. Silva[3], M. Li[4], D. A. Lowther[5]

Computational Electromagnetics Lab, Dept. of ECE, McGill University, Montreal, QC, H3A 0E9 Canada
mhmohammadi@ieee.org[1], tanvir.rahman@mcgill.ca[2], rodrigo.silva@mail.mcgill.ca[3],
min.li@mail.mcgill.ca[4], david.lowther@mcgill.ca[5]

A computationally efficient algorithm for rotor design optimization of Synchronous Reluctance Machines (SynRMs) has been proposed. A mixed-integer design space of rotor pole numbers and single barrier rotor geometry was considered to develop a generalizable algorithm for carrying out multi-objective design and optimization of SynRMs. By using 2D FEA time-stepping simulations, two objective values per sampled design were generated: average torque and torque ripple. Non-linear regression analysis using the Bayesian Regularization Backpropagation Neural Network (BRNN) was used to train surrogate models for the two design objectives. A convergence criterion of 20 neurons for the hidden layer size was observed per objective. The resulting Response Surface (RS) models were then used to calculate a Pareto front in the objective space through Genetic Algorithm (GA) optimization.

***Index Terms*— AC motors, finite element analysis, genetic algorithms, neural networks, Pareto optimization, surrogate modelling**

I. Introduction

RESEARCH and development of hybrid and electric vehicles (HEVs) has been promising in recent years: both traditional and new vehicle manufacturers aim to reduce carbon emissions and fuel consumption in the transportation industry over the next decades. Because of high torque-to-rotor volume density, rare earth permanent magnet motors have been the accepted choice so far for applications in the automotive sector. However, recent fluctuations in the price and supply of rare earth materials has led to vigorous research activities on motor topologies which use either less or no rare-earth magnet material while sustaining efficiency and performance requirements [1].

One possible candidate is the Synchronous Reluctance Machine (SynRM) which produces electromagnetic reluctance torque through variations in the rotor inductances due to flux barriers and carriers. Even though the geometric placement of flux barriers and carriers is crucial for selecting a high-performance machine, exploring the motor's design space through Finite-Element Analysis (FEA) for a global optimal can be both problematic and computationally expensive [2]. First, the design variables can be both discrete (e.g. number of rotor poles, number of stator slots, winding configurations, etc.) or continuous (e.g. flux barrier width and other geometric dimensions) leading to an NP-hard mixed-integer problem [3]. Next, the number of optimization objectives and the design space dimensions both impact the computational time needed to generate the Pareto front of optimal solutions.

Therefore, this paper discusses an efficient algorithm for addressing the computational challenges in designing a SynRM through a case study with a single barrier and different possible rotor pole integer numbers. The global optimization problem was solved using non-linear regression analysis, also known as surrogate modelling, of a sampled design space consisting of discrete and continuous variables. As explained under Section II, this is the first application for developing computationally efficient design algorithms for SynRMs.

II. Proposed Algorithm

The proposed flowchart for the optimal Pareto designs of a single barrier SynRM rotor is illustrated in Fig. 1 (left). A *3-phase 33-slot* stator, with stator outer diameter OD_s *325mm* and motor stack length L_{stk} *275mm*, was fixed for all rotor geometrical variations and has been employed from a direct-drive application. Each subsection explains the flowchart steps using the SynRM case study: (A) Geometric Modeling, (B) Data Acquisition, (C) Surrogate Modelling and (D) Multi-Objective Optimization. Once the Pareto front was obtained, the optimal design solutions were validated using FEA solves to compare the relative error differences.

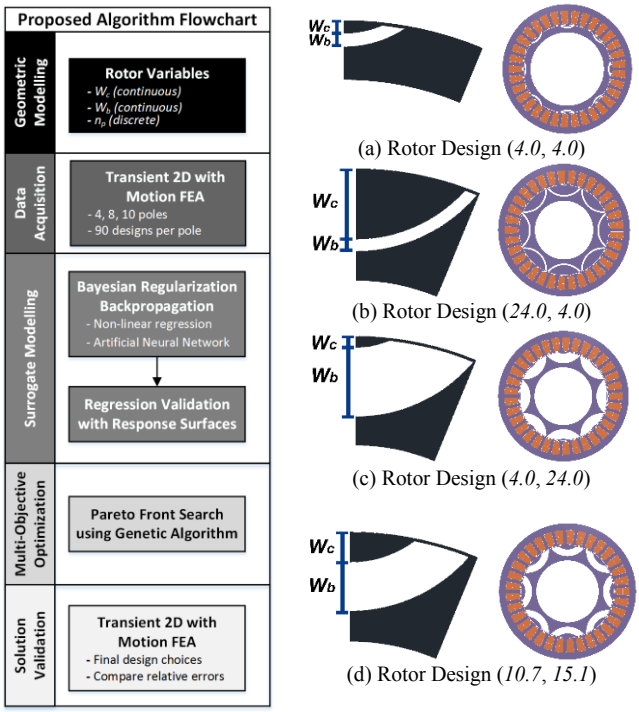

(a) Rotor Design (*4.0*, *4.0*)

(b) Rotor Design (*24.0*, *4.0*)

(c) Rotor Design (*4.0*, *24.0*)

(d) Rotor Design (*10.7*, *15.1*)

Fig. 1. Left: Proposed Flowchart for Optimal SynRM Rotor Design, Right: Sample *8-Pole* Rotor Designs for (W_c, W_b) in *mm*

A. Geometric Modelling

For the fixed stator, the rotor flux carrier W_c and barrier W_b widths were modelled using the intersections of different circular radii from a fixed center. Each width ranges from a lower bound to a maximum limit W_{lim} for *4, 8* and *10 poles*: this ensures that two adjacent poles do not intersect for each pole number n_p as constrained in (1). Hence, the design space consists of *3* dimensions. The flux barrier consists of air, and the stator and rotor core material used is *M-19 29 Ga* steel. For each n_p, the design space was sampled using a full factorial approach due to the low number of dimensions. Fig. 1 (right) illustrates four different rotor designs for the *8-pole* case.

$$W_c + W_b \leq W_{lim} \tag{1}$$

B. Data Acquisition

Since the chosen L_{stk} is relatively long with respect to OD_s, 2D FEA solves can estimate the motor's performance while neglecting end effects. Stator windings operated at *150%* rated current ($350A_{rms}$), and the current advance angle was varied to obtain the Maximum-Torque-Per-Ampere point within $\pm 1°$. For every rotor design, a Transient 2D with Motion FEA was solved for $1/6^{th}$ of a rotor revolution and *48* sample points to obtain a steady-state waveform graph of instantaneous torque T [4]. The two evaluated objectives for each motor design were average torque T_{avg} (2) and torque ripple T_{rip} (3).

$$T_{avg}(W_c, W_b) = \frac{1}{N}\sum_{i=1}^{N} T_i \qquad [N{\cdot}m] \tag{2}$$

$$T_{rip}(W_c, W_b) = \frac{|\max(T) - \min(T)|}{T_{avg}(W_c, W_b)} \qquad [\%] \tag{3}$$

C. Surrogate Modelling

Upon FEA data acquisition, the entire dataset (n_p, W_c, W_b) was used to train two objective networks (T_{avg}, T_{rip}) using the Bayesian Regularization Backpropagation Neural Network (BRNN) with a single hidden layer through [5]-[6]. This training function can handle the tradeoff of over-fitting and trend generalization. The training, validation, testing sets were randomly divided into *60%*, *25%*, *15%* of the initial dataset. For training T_{avg} and T_{rip}, the number of neurons was increased up to *20* until the convergence was met as presented in Table I. The *8-pole* Response Surface (RS) maps are shown in Fig. 2.

TABLE I
CORRELATION COEFFICIENT R^2 FOR THE TRAINED 8-POLE BRNN

Objective	*Training*	*Validation*	*Testing*
T_{avg}: Average Torque	*1.0000*	*0.9998*	*0.9999*
T_{rip}: Torque Ripple	*0.9969*	*0.9578*	*0.9684*

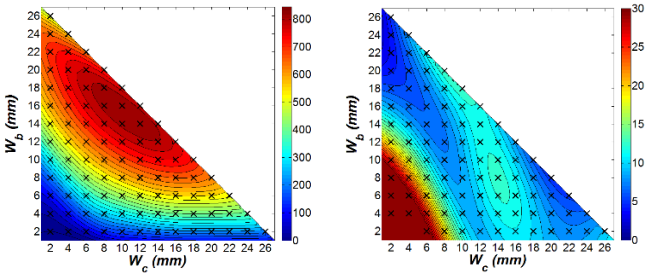

Fig. 2. BRNN RS Maps of T_{avg} in *Nm* (left) and T_{rip} in *%* (right) for *8 poles* in (W_c,W_b) Plane: crosses correspond to sampled design space points

D. Multi-Objective Optimization

Lastly, a Pareto optimization using Genetic Algorithm (GA) was employed by maximizing T_{avg} while minimizing T_{rip}. The initial population was evenly divided between *4*, *8* and *10-pole* datasets. The crossover function was chosen to handle both discrete and continuous variables. As in [7]-[8], the use of a surrogate model (BRNN) with GA can reduce the computation overhead in function evaluations. The final Pareto front in Fig. 3 only consists of *8-pole* solutions, since the RS map of T_{rip} has smaller values than the *4-* and 10-*pole* numbers.

III. RESULT VALIDATION AND DISCUSSION

All the final Pareto front solutions were validated using the FEA solves similar to Section II-B. The acceptable relative error percentage statistics for the Pareto front are presented on Fig. 3. Due to the tradeoffs between over-fitting and trend generalization of the input dataset, the high-frequency values in T_{rip}'s dataset led to higher errors than in T_{avg}. This is also demonstrated through the differences in R^2 values between the two objectives in Table I. In conclusion, this proposed algorithm can effectively address mixed-integer problems which commonly occur in motor design problems. The final design choices may then be passed on to the motor designer to effectively select a suitable solution from the Pareto front.

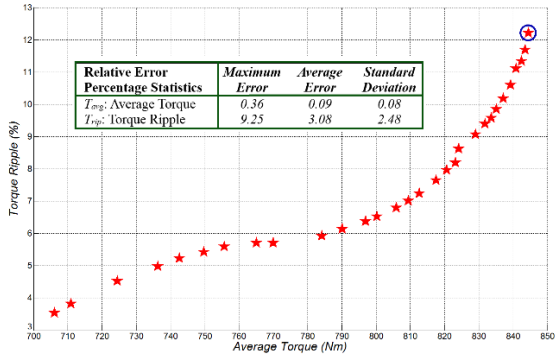

Fig. 3. Final Pareto Front and Relative Error Percentages with respect to Validated FEA Solutions: circled point corresponds to design (d) in Fig. 1

IV. REFERENCES

[1] I. Boldea, L. Tutelea, L. Parsa, and D. Dorrell, "Automotive Electric Propulsion Systems with Reduced or No PMs: An Overview," *IEEE Trans. Ind. Electron.*, vol. 61, no. 10, pp. 5696-5711, Oct. 2014.

[2] G. Pellegrino, C. Cupertino, F. Gerada, "Automatic Design of Synchronous Reluctance Motors focusing on Barrier Shape Optimization", *IEEE Trans. Ind. Appl.*, no. 99, Aug. 2014.

[3] S. Burer, and A. N. Letchford, "Non-Convex Mixed-Integer Nonlinear Programming: A Survey," *Surveys in Operations Research and Management Science*, vol. 17, no. 2, pp. 97-106, Jul. 2012.

[4] Infolytica MagNet and MotorSolve BLDC: 2D/3D Electromagnetic Field Simulation Software. Available: www.infolytica.com. Dec. 2014.

[5] D. J. C. MacKay, "Bayesian Interpolation," *Neural Computation*, vol. 4, no. 3, pp. 415–447, May 1992.

[6] F. D. Foresee, and M. T. Hagan, "Gauss-Newton approximation to Bayesian regularization," *Proc. Int. Joint Conf. Neural Networks*, vol. 3, pp. 1930–1935, 9-12 Jun. 1997.

[7] S. Giurgea, H. S. Zire, and A. Miraoui, "Two-Stage Surrogate Model for Finite-Element-Based Optimization of Permanent-Magnet Synchronous Motor," *IEEE Trans. Magn.*, vol.43, no.9, pp.3607-3613, Sep. 2007.

[8] G. Crevecoeur, P. Sergeant, L. Dupre, and R. Van de Walle, "A Two-Level Genetic Algorithm for Electromagnetic Optimization," *IEEE Trans. Magn.*, vol.46, no.7, pp.2585-2595, Jul. 2010.